Space Rendezvous Laboratory
Department of Aeronautics and Astronautics
Stanford University
https://slab.stanford.edu/

Orbit Design and Control for the Earth-Orbiting Starshade Mission

Adam Koenig and Simone D'Amico

September 30, 2019

Technical Report No: TN-19-02

Contents

Scope

An Earth-orbiting starshade has been recently proposed by Dr. John Mather to take the first ever images of Earth-like planets around Sun-like stars. The baseline mission uses a 100m-diameter starshade flying approximately 200000km from a ground telescope during observations (e.g., from Mauna Kea or Chile) resulting in an inner working angle of 50milliarcsec. The starshade will produce a cylindrical shadow approximately 40m in diameter perpendicular to the line of sight and a few thousands of kilometers in length. To ensure that telescopes such as the Extremely Large Telescope (ELT) are entirely contained within the shadow during observations, the position of the starshade will have to be controlled to within $\pm$2m perpendicular to the line of sight and a few thousands of kilometers along the line of sight during observations. The orbit of the starshade must be selected to allow at least three observations of each target star to enable determination of the orbit of an observed planet. Additionally, the mission must observe as many targets as possible to maximize the science return. Accordingly, it is desirable to select the orbit and operations strategy to minimize propellant consumption.

To meet this need, this technical note augments a set of provided optical requirements with a set of orbit requirements to ensure safety and repeatability of observations. These requirements are used to 1) bound the feasible design space for the mission, 2) identify optimal configurations of the starshade orbit, telescope location, and observation times for an arbitrary target star, and 3) quantitatively characterize the required thrust levels, delta-v budgets, and propellant mass budgets for all mission activities. The propellant mass budgets are analyzed for both monolithic and distributed mission architectures for completeness.

Following this introduction, the optical requirements for the mission are provided in Section 1. These optical requirements are translated into constraints on the mission design in Section 2. Using these constraints, the optimal starshade orbit(s) for observation of a specified target are derived in Section 3 along with the required delta-v and thrust. Next, Section 4 derives constraints on the observation geometry that ensure that the minimum perigee altitude requirement is always satisfied. Section 5 describes a novel orbit reconfiguration strategy that reduces the delta-v cost of large plane changes and Section 6 demonstrates that significant propellant mass savings can be achieved by using a distributed mission architecture consisting of a minimalistic starshade spacecraft and a servicer spacecraft carrying the required propellant. Finally, conclusions and next steps are summarized in Section 7.

1 Mission Requirements

The proposed mission concept imposes eight fundamental requirements that must be met throughout all observations:

REQ 1: The normal vector to the starshade plane shall be within 20deg of parallel to the line of sight from the telescope to the target star.
Rationale: This ensures that the shadow produced by the target is deep enough to enable imaging of exoplanets while maximizing the range of compliant observation geometries.

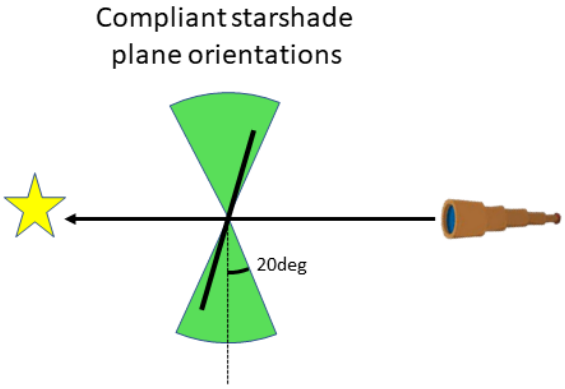

Figure 1: Illustration of REQ 1.

REQ 2: The target-facing normal vector to the starshade plane shall be within 89deg of the pointing vector to the sun.
Rationale: This ensures that the telescope-facing side of the starshade (including supporting structures) is not illuminated by the sun.

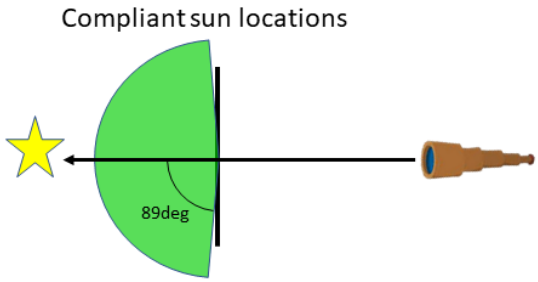

Figure 2: Illustration of REQ 2.

REQ 3: The pointing vector to the sun shall be at least 18deg below the horizon as seen by the telescope.

Rationale: This ensures that scattered sunlight in the atmosphere does not degrade images collected by the telescope.

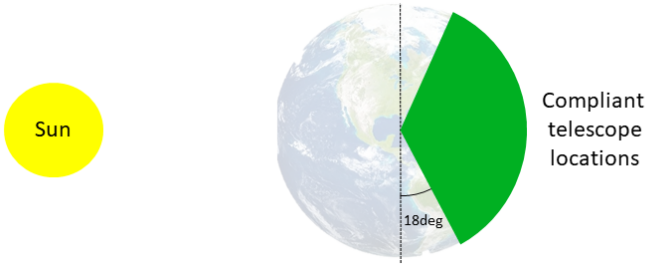

Figure 3: Illustration of REQ 3.

REQ 4: The telescope shall be pointed within 60deg of its local zenith direction.
Rationale: This ensures that the telescope views at airmasses of less than two.

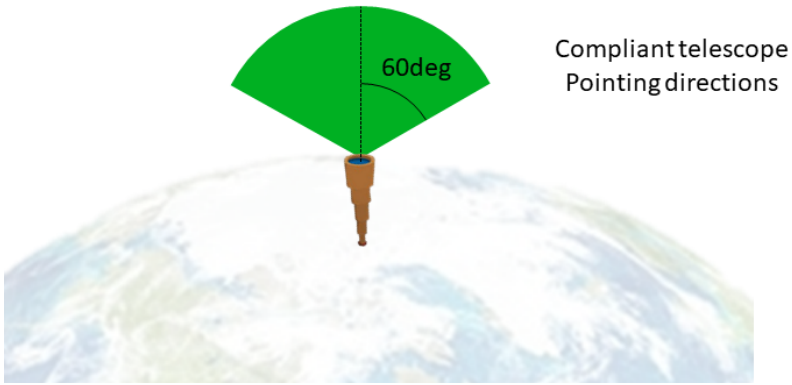

Figure 4: Illustration of REQ 4.

REQ 5: The starshade orbit shall be commensurable to the sidereal day.
Rationale: This ensures that observations can be repeated with identical formation geometry.

REQ 6: The orbit perigee shall have an altitude of at least 1000 km.
Rationale: This ensures that the starshade does not reenter the atmosphere in the event of an anomaly in the propulsion system and minimizes risk of collision with debris in low orbit.

REQ 7: The center of the starshade shall remain within ±2m of the line of sight from the telescope to the target star.
Rationale: This ensures that the telescope aperture is entirely within the shadow produced by the starshade.

REQ 8: The separation between the telescope and starshade shall remain within 1% of a specified baseline separation (nominally 200000km).
Rationale: This ensures that the telescope is within the shadow produced by the starshade.

2 Design Constraints

For each observed target, these requirements must be met through proper selection of twelve design variables: the orbit of the starshade (6 variables), the orientation of the starshade (3 variables), the latitude of the observing telescope, the time of year that the target is observed, and the time of day that the target is observed. However, as will be demonstrated in the following, the requirements result in strict constraints on these variables.

REQ 1 stipulates that the plane of the starshade must be perpendicular to the line of sight to within 20deg and REQ 2 requires that the sun illuminates the target-facing side of the starshade. Combining these requirements, the orientation of the starshade is effectively fixed by the location of the target and the location of the sun. Specifically, the starshade should be oriented perpendicular to the line of sight to the target and tilted only enough to ensure that the telescope-facing side of the starshade is not illuminated to maximize the depth of the shadow. Another immediate consequence of these requirements is that a target can only be observed when its line of sight is within 109deg of the pointing vector to the sun.

REQ 3 stipulates than the sun must be below the horizon to prevent scattered light in the atmosphere from degrading collected images. It follows that the telescope can only observe a target at night, nominally between 7:15PM and 4:45 AM local solar time.

REQ 4 constrains the set of targets that can be viewed at any specific time to be within 60deg of the local zenith direction.

The relationships between the constraints imposed by REQs 1-4 for a telescope located at the equator are shown in Figure 5. Two important conclusions can be drawn from

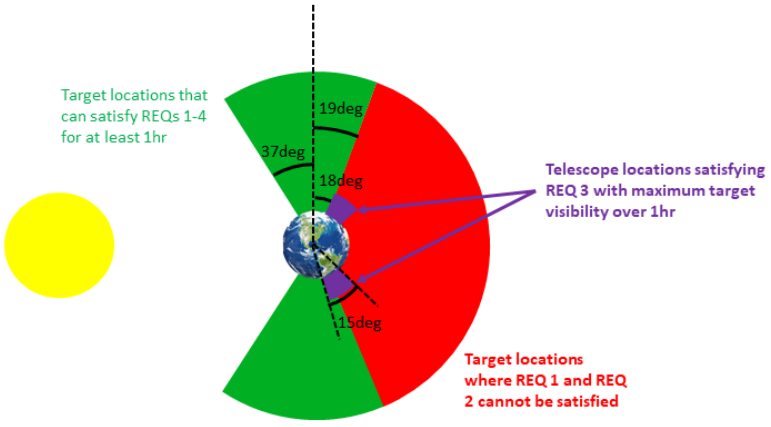

Figure 5: Relationship between constraints imposed by optics requirements.

this Figure. First, observations should be conducted in the 1hr window adjacent to a

violation of REQ 3 (e.g. 7:15-8:15PM or 3:45-4:45AM local solar time), to maximize the number of available targets. Second, the best time of year to observe a given target is when the pointing vector to the sun is nearly perpendicular to the pointing vector to the target. This maximizes the size of the time windows in which all four requirements are satisfied simultaneously. The authors note that this behavior is latitude dependent (i.e. there exist large windows where a telescope at high latitude can observe a target near the celestial pole). However, it will be demonstrated in later analysis that such scenarios are undesirable from a safety perspective, so these trends hold for most realistic mission profiles.

Thus far, REQs 1-4 have imposed strict constraints on the relationships between the target location, time of year, time of day, and starshade orientation during observations. The remaining requirements must be met through proper selection of the telescope latitude and starshade orbit (7 variables).

REQ 5 stipulates that the orbit period must be commensurable with the sidereal day. This means that there exist integers m and n such that

$$nT_{sid} = mT \tag{1}$$

where T_{sid} is the duration of a sidereal day (86164s) and T is the orbit period. The semimajor axis a can be computed as a function of these variables given by

$$a = \sqrt[3]{\frac{\mu n^2 T_{sid}^2}{4m^2\pi^2}} \approx 42164\text{km}\left(\frac{n}{m}\right)^{2/3} \approx \left\{\begin{matrix} 106247\text{km} & n=4 & m=1 \\ 123289\text{km} & n=5 & m=1 \\ 139223\text{km} & n=6 & m=1 \\ 154291\text{km} & n=7 & m=1 \\ \dots & \dots & \dots \end{matrix}\right\} \tag{2}$$

Because the ratio n/m must be $\geq$4 to achieve a large enough semimajor axis to accommodate the nominal separation of 200000km between the telescope and starshade, it is evident that the optimal choice of m is 1 to maximize observation frequency. However, n is subject to conflicting objectives. It is desirable to maximize n to minimize the delta-v cost of reconfiguration maneuvers to observe different targets. At the same time, it is desirable to minimize n to maximize the frequency of repeat observations.

Next, REQ 6 stipulates that the orbit must always have a perigee altitude of at least 1000km to ensure that the starshade does not reenter earth's atmosphere in the event of an anomaly in the propulsion system and minimize the risk of collision with debris in low orbit. This poses a constraint on the eccentricity and semimajor axis given by

$$a(1-e) \geq R_E + 1000\text{km} = 7378\text{km} \tag{3}$$

Finally, REQ 7 and REQ 8 specify the accuracy with which the starshade must follow the telescope. For simplicity, it is hereafter assumed that the starshade tracks the position and velocity of the telescope in the plane perpendicular to the line of sight exactly. This is accomplished by continuously maneuvering to negate the relative acceleration in this plane. The 1% tolerance in separation along the line of sight is assumed based on tolerances from previous studies [1, 2, 3, 4]. These requirements result in tight constraints on the relative position of the starshade with respect to the telescope as well as the relative velocity in the plane perpendicular to the line of sight. However, the relative velocity along the line of sight can be as large as 1km/s while ensuring that the separation tolerance is not violated throughout a 1hr observation. There are multiple values within this range that provide a orbit semimajor axis that satisfies the condition in Eq. (2) to enable repeated observations. Thus, the orbit of the starshade is almost fully specified by the position and velocity of the telescope at the start of the observation, the required separation between the telescope and starshade, and the orbit semimajor axis. The single ambiguity lies in the sign of the relative velocity along the line of sight, which can be exploited to minimize the delta-v cost of aligning the starshade with different targets. Figure 6 shows pairs of orbits with different periods that can be used to observe a reference target with a right ascension of 90deg and a declination of 45deg. These orbits are shown in an earth-centered inertial (ECI) frame with the origin at the center of the earth.

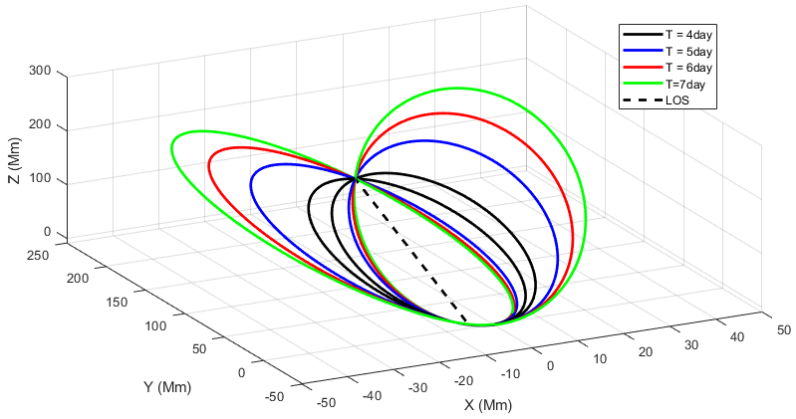

Figure 6: Illustration of orbits with periods from 4-7 days that provide proper alignment with a reference target with a right ascension of 90deg and a declination of 45deg for a nominal separation of 200Mm between the starshade and telescope.

Combining these results, the feasible design space is constrained by three rules:

1. Observations should be conducted shortly after 7:15PM or before 4:45AM local solar time to maximize the number of available targets for the telescope
2. The time of year should be selected such that the pointing vector to the sun is nearly perpendicular to the pointing vector to the target to ensure the existence of windows where all optical requirements are satisfied.

3. The orbit of the starshade is specified by the position and velocity of the telescope at the start of the observation. The relative velocity along the line of sight is selected to provid the desired orbit period (see Eq. 2).

3 Optimal Orbits for Station-Keeping

The previous section provided bounds to the design space to ensure that all optical requirements can be satisfied simultaneously. Within this feasible design space, it is desirable to identify optimal configurations that minimize the delta-v cost required for station-keeping during observations.

The fundamental requirements posed by the mission concept are that the position of the starshade ($\boldsymbol{r}_S$) must maintain a nearly constant offset from the position of the telescope ($\boldsymbol{r}_T$) and the components of the velocity of the starshade ($\boldsymbol{v}_S$) and the velocity of the telescope ($\boldsymbol{v}_T$) in the plane perpendicular to the line of sight must be equal. These requirements are met by having the starshade perform maneuvers that counteract the difference between the accelerations of the starshade ($\boldsymbol{a}_S$) and telescope ($\boldsymbol{a}_T$) in the plane perpendicular to the line of sight. As demonstrated in previous works [2, 3, 4, 5, 6], this operations concept results in substantial delta-v savings as compared to the cost of counteracting the full relative acceleration.

To simplify the following analysis, it is helpful to describe the motion of the telescope and starshade in the L-frame, which is defined by unit vectors along the line-of-sight (first axis) and the telescope's geographic parallel in east direction (second axis) as shown in Figure 7. The third axis of L completes the right-handed triad. If the line-of-sight points in zenith direction, the third axis of L is aligned with the telescope's meridian in north direction.

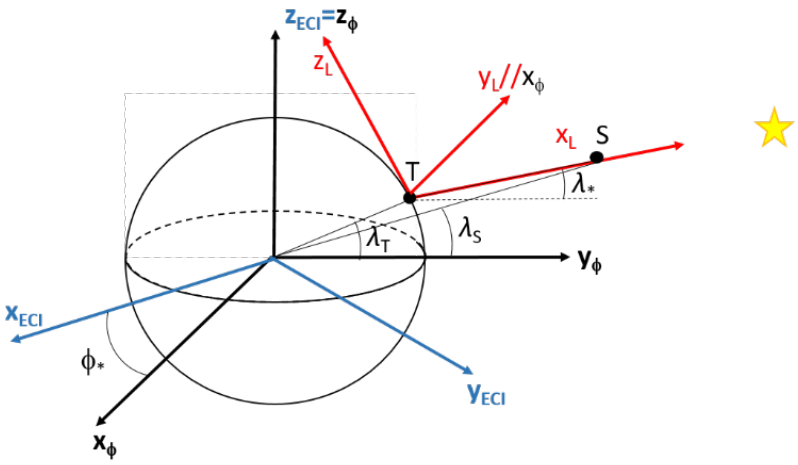

Figure 7: Visualization of coordinate frames including Earth-Centered Inertial (blue, ECI) frame, line-of-sight (red, L) frame, and frame aligned with longitude of telescope/starshade/target star (black, ϕ). S and T stand for starshade spacecraft and telescope.

The acceleration of the telescope in the L-frame ($\boldsymbol{a}_{T_L}$) is given as follows

$$\boldsymbol{a}_{T_L} = \omega^2 r_T \cos\lambda_T \begin{bmatrix} -\cos\lambda_* \cos\omega t \\ -\sin\omega t \\ \sin\lambda_* \cos\omega t \end{bmatrix} \tag{4}$$

where λ_T is the latitude of the telescope, λ_* is the declination of the target star, ω is earth's angular velocity, and t represents the time elapsed from a configuration where the longitude of the telescope matches the longitude of the target star as measured from the same reference direction (e.g., vernal equinox). The second and third components of Eq. 4 give the telescope's acceleration perpendicular to the line-of-sight and can be combined to provide

$$a_{T_\perp}(t) = \omega^2 r_T \cos\lambda_T \sqrt{\sin^2\omega t + \sin^2\lambda_* \cos^2\omega t} \tag{5}$$

It is evident from this equation that the acceleration of the telescope perpendicular to the line of sight decreases with $|\lambda_T|$ and increases with λ_* and $|t|$. Also, the acceleration is minimal when telescope and target star longitudes are equal (i.e., $t = 0$). It follows that observations should be conducted as close as possible to the time at which the telescope longitude is equal to the target longitude to minimize delta-v costs.

It is noted that no approximations have been introduced to derive Eq. 5 except that earth has a constant angular momentum vector. Since the term in the square root in Eq. 5 can be no larger than one, the acceleration perpendicular to the line of sight is bounded by

$$a_{T_\perp} \leq \omega^2 r_T \cos\lambda_T = 33.7\text{mm/s}^2 \cdot \cos\lambda_T \tag{6}$$

Next, the acceleration of the starshade is given as

$$\boldsymbol{a}_S = -\mu \frac{\boldsymbol{r}_S}{r_S^3} \tag{7}$$

Because the starshade orbit radius must be at least 200000km during observations, the magnitude of the starshade acceleration a_S is bounded by

$$a_S \leq \frac{\mu}{200000\text{km}^2} \approx 0.01\text{m/s} \tag{8}$$

Also, the angle between this acceleration and the line of sight β is bounded by

$$\beta \leq \frac{r_T}{200000\text{km}} \approx 0.032\text{rad} \tag{9}$$

Combining Eqs. 8 and 9, the component of the acceleration of the starshade perpendicular to the line of sight $a_{S_\perp}$ is bounded by

$$a_{S_\perp} \leq a_S \sin\beta \approx 0.32\text{mm/s}^2 \tag{10}$$

It is clear from this bound that the acceleration of the starshade perpendicular to the line of sight is negligible as compared with the telescope's acceleration (two orders of magnitude less) and can be reasonably neglected in computation of the station-keeping delta-v cost.

Combining these results leads to a simple analytic formula for the total delta-v required for an observation of duration Δt which starts at an arbitrary time t_0 from the configuration of equal longitudes of telescope and star (i.e., $t = 0$). This delta-v is computed by integrating the acceleration perpendicular to the line of sight in Eq. 5 as given by

$$\Delta v = \omega^2 r_T \cos\lambda_T \int_{t_0}^{t_0+\Delta t} \sqrt{\sin^2\omega t + \sin^2\lambda_* \cos^2\omega t}\, dt \tag{11}$$

Because the argument of the integral varies between $|\sin\lambda_*|$ and 1, it is evident that the delta-v cost of an observation is bounded by

$$\Delta v \leq \omega^2 r_T \cos\lambda_T \Delta t \approx 121.4\text{m/s} \cdot \cos\lambda_T \tag{12}$$

The most important features of this bound are that it is linear in time and proportional to the cosine of the telescope latitude. Also, because the argument of the integral in Eq. 11 varies slowly with time, the delta-v cost of a short observation ($\leq$1hr) can be approximated using a single step Euler integration as given by

$$\Delta v = \omega^2 r_T \cos\lambda_T \Delta t \sqrt{\sin^2\omega t_c + \sin^2\lambda_* \cos^2\omega t_c} \tag{13}$$

where t_c is the epoch in the middle of the observation (i.e. $t_c = t_0 + \Delta t/2$).

The approximation in Eq. 13 was validated through comparison to numerical integration of the cost in Eq. 11. The delta-v costs computed analytically and numerically for 1hr observations of targets with declinations from -90deg to 90deg for selected values of t_c are shown in Figure 4 for an equatorial telescope. Because t_c defines the right ascension of the target for a given observation date, this plot also characterizes the sensitivity of the delta-v cost to the location of the target.

Two important conclusions can be drawn from this plot. First, the analytical model in Eq. 13 provides an accurate approximation of the true delta-v cost of an observation. Indeed, the difference between the analytical and numerical models is no larger

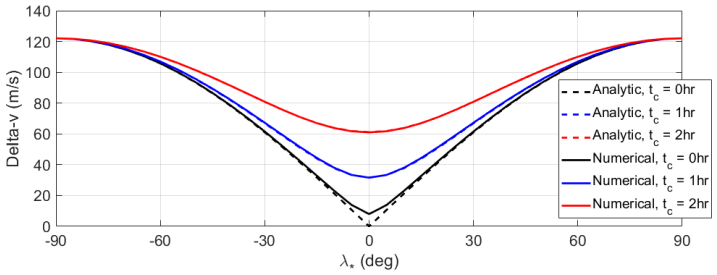

Figure 8: Analytic and numerical delta-v cost of 1hr observation for telescope on equator vs target declination for selected t_c.

than 10m/s in all test cases. The maximum error is observed when the declination of the target star is less than 5deg and t_c ¡ 20min. However, these errors are negligible for mission planning purposes because few (if any) observations will satisfy these conditions. Thus, the delta-v for orbit keeping activities can be computed analytically based on the telescope's latitude, target stars' latitude, and the start times and durations of planned observations. Second, it is evident that targets near the equator can be observed at reduced delta-v cost as predicted. This benefit is maximized if t_c = 0hr, which centers the observation about the point when the telescope and target longitudes are equal. However, a 2hr offset only increases the delta-v cost to half of the cost of observing a polar target.

The thrust required to execute the described maneuvers is equal to the product of the mass of the spacecraft and the largest relative acceleration perpendicular to the line of sight throughout the mission lifetime. The instantaneous thrust required to negate the relative acceleration perpendicular to the line of sight is given by

$$F = m_S \omega^2 r_T \cos\lambda_T \sqrt{\sin^2 \omega t + \sin^2 \lambda_* \cos^2 \omega t} \tag{14}$$

where m_S is the mass of the starshade spacecraft. Because the square root term cannot exceed one, the thrust is bounded by

$$F \leq 0.0337\text{m/s}^2 \cdot m_S \cos\lambda_T \tag{15}$$

For a reference spacecraft with a mass of 20 metric tons and an equatorial telescope, a worst-case observation will require a thrust of 674N. However, it is likely that the telescope will have to be shuttered during thruster activities to prevent the light from the thrust plume from degrading images. To ensure that a worst-case observation can be performed with a thruster duty cycle no larger than 10%, the starshade spacecraft will need approximately 7000N of available thrust. The required thrust level excludes the usage of high specific impulse propulsion technology such as solar electric propulsion (SEP) and forces the usage of chemical propulsion for station-keeping

maneuvers. However, as will be demonstrated in the following sections, the delta-v cost of station-keeping maneuvers are within an order of magnitude of the total delta-v cost of the mission. Thus, the propellant mass budget will be driven by orbit keeping activities because the specific impulse of SEP propulsion is at least ten times larger than the specific impulse of a chemical propulsion system. Additionally, it is evident that the required propellant mass is minimized if chemical propulsion is only used for station-keeping during observations and SEP is used for all reconfigurations (including re-aligning with the same target and aligning with different targets).

4 Passive Safety Constraints

The analysis in the previous section demonstrated that the delta-v cost of orbit keeping and the required thrust scale with the cosine of the latitude of the telescope. It follows that the telescope latitude should be maximized to reduce the mission delta-v cost, thereby maximizing the number of targets that can be observed. However, it will be demonstrated in the following that there is a maximum telescope latitude at which any given target can be observed while ensuring that the minimum perigee altitude requirement (REQ 6) is met.

To ensure that observations can be repeated once per orbit, the orbit semimajor axis must satisfy the condition in Eq. 2. Also, the orbit must have a sufficiently large angular momentum to ensure that the minimum perigee radius requirement is satisfied ($r_p \geq 7378$km). The minimum specific angular momentum (h_{min}) required to ensure that the perigee radius requirement is met can be expressed as a function of a as given by

$$h_{min} = \sqrt{\mu a\Big(1 - \Big(1 - \frac{r_p}{a}\Big)^2\Big)} = \sqrt{\mu\Big(14756\text{km} - \frac{(7378km)^2}{a}\Big)} \tag{16}$$

Over a semimajor axis range of 100-150Mm, h_{min} remains within one percent of $7.55 \times 10^{10}\text{m}^2/\text{s}$. During the described observation profile, the position ($\boldsymbol{r}_{T_L}$) and velocity ($\boldsymbol{v}_{T_L}$) of the telescope in the L-frame follow a trajectory given by

$$\boldsymbol{r}_{T_L} = r_T \cos\lambda_T \begin{bmatrix} \cos\lambda_* \cos\omega t \\ \sin\omega t \\ -\sin\lambda_* \cos\omega t \end{bmatrix} \qquad \boldsymbol{v}_{T_L} = \omega r_T \cos\lambda_T \begin{bmatrix} -\cos\lambda_* \sin\omega t \\ \cos\omega t \\ \sin\lambda_* \sin\omega t \end{bmatrix} \tag{17}$$

And the position ($\boldsymbol{r}_{S_L}$) and velocity ($\boldsymbol{v}_{S_L}$) of the starshade are given by

$$\begin{aligned} \boldsymbol{r}_{S_L} &= r_T \cos\lambda_T \begin{bmatrix} \cos\lambda_* \cos\omega t \\ \sin\omega t \\ -\sin\lambda_* \cos\omega t \end{bmatrix} + \begin{bmatrix} d \\ 0 \\ 0 \end{bmatrix} \\ \boldsymbol{v}_{S_L} &= \omega r_T \cos\lambda_T \begin{bmatrix} -\cos\lambda_* \sin\omega t \\ \cos\omega t \\ \sin\lambda_* \sin\omega t \end{bmatrix} + \begin{bmatrix} \dot{d} \\ 0 \\ 0 \end{bmatrix} \end{aligned} \tag{18}$$

where d is the nominal separation between the starshade and telescope and $\dot{d}$ is the drift rate along the line of sight, which is selected to provide the desired semimajor axis. The angular momentum of the orbit h is given as

$$h = ||\boldsymbol{r}_{S_L} \times \boldsymbol{v}_{S_L}|| \tag{19}$$

Because $d \gg r_T$, this cross product can be approximated as

$$h = dr_t\omega \cos\lambda_T \sqrt{\cos^2\omega t + \sin^2\lambda_* \sin^2\omega t} \tag{20}$$

To ensure that $h \geq h_{min}$, the latitude of the telescope must be selected to satisfy

$$\cos\lambda_T \geq \frac{h_{min}}{dr_T\omega} \approx 0.8117 \tag{21}$$

For a nominal d of 200000km, the maximum latitude of the telescope is 35.7deg. Within this latitude range it is still necessary to ensure that the target latitude and time at which the observation is conducted are selected to satisfy the constraint given by

$$\sqrt{\cos^2\omega t + \sin^2\lambda_* \sin^2\omega t} \geq \frac{h_{min}}{dr_T\omega\cos\lambda_T} \tag{22}$$

Figure 9 shows the maximum $|t|$ that satisfies this constraint as a function of the target declination for selected telescope latitudes from 0deg to 30deg. Two important conclusions can be drawn from this plot. First, while equatorial targets exhibit the lowest delta-v cost per hour of observation, this property comes with tight constraints on observation times that satisfy the minimum perigee radius requirement. The effect of these constraints is most significant for telescopes at high latitude (≥30deg). This constraint also limits the number of repeated observations that can be performed on a near-equatorial target because the difference between solar and sidereal time increases by 4min per day (and at least 16min per orbit). The second conclusion that can be drawn from this plot is that targets with high declination (≥60deg) can be observed at any time (provided the optical constraints are satisfied).

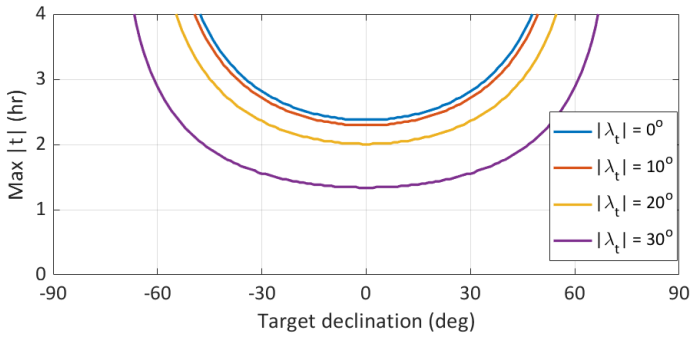

Figure 9: Maximum $|t|$ satisfying minimum perigee altitude constraint vs target declination for selected telescope latitudes.

5 Orbit Reconfiguration Analysis

A key challenge for the earth orbiting starshade mission concept is the need to perform large orbit reconfigurations to allow observations of different targets with large angular separations. Preliminary analysis using an optimal impulsive maneuver planning algorithm [7] found that rotating the starshade orbit with a period of four days incurs a delta-v cost of 30m/s per degree. At this rate, rotating the orbit plane by 60 degrees to observe a new target would cost 1800m/s. This delta-v cost is unrealistic for two reasons. First, the spacecraft would have to be refueled after observations of one or two target stars. Second, the baselined SEP propulsion system (4N thrust, assumed 20000kg mass) is only capable of providing 60m/s delta-v per week operating at 50% duty cycle. At this rate, each reconfiguration would take 30 weeks, resulting in observations of fewer than two targets per year. One means of reducing this delta-v cost is to increase the period of the orbit. Increasing the orbit period to 15 days reduces the delta-v cost to 20 m/s per degree, but this is still unrealistically expensive and significantly reduces the number of observations that can be performed for each target star.

Due to these limitations, it is evident that a more delta-v efficient orbit reconfiguration strategy is needed to enable the earth-orbiting starshade mission concept. Specifically, it is desirable to provide large orbit reconfigurations (up to 60deg) with a delta-v cost of 720m/s or less to enable reconfigurations in three months or less with the proposed solar electric propulsion system. This would enable observation of 4 targets per year and reduce the number of times the spacecraft must be refueled.

To meet this need, a reconfiguration strategy hereafter called "deep space reconfiguration" is analyzed in the following. This analysis is intended to serve as a proof-of-concept that quantitatively characterizes the achievable delta-v savings using this approach. With this in mind, it is assumed that all maneuvers are impulsive. More detailed considerations such as low-thrust maneuver planning and inclusion of perturbations are left to future work.

The deep space reconfiguration strategy leverages the fact that the orbit only needs to be rotated allow observations of different targets (i.e. the size and shape are nearly constant). The delta-v cost of such reconfigurations can be minimized by performing maneuvers when the orbit radius is as large as possible. To maximize the orbit radius during plane change maneuvers, orbit reconfigurations are performed using the sequence of four maneuvers described in the following.

The first maneuver, called the ascent maneuver, is executed in the flight direction at the first perigee pass after the final observation of a specified target. This maneuver places the starshade in an intermediate orbit with a much larger apogee radius, allowing for more efficient maneuvers to change the orientation. The second and third maneuvers, called the entry and exit maneuvers, rotate the intermediate orbit such that the perigee coincides with the perigee of the orbit required to observe the next

target. Finally, the fourth maneuver, called the descent maneuver, is executed in the anti-flight direction at the next perigee pass. This maneuver lowers the apogee radius, achieving the required orbit for observation of the next target. The main advantage of this approach is that the reduction in cost of the maneuvers to change the orbit orientation is larger than the delta-v cost of the ascent and descent maneuvers for large reconfigurations. A notional trajectory produced by this maneuver sequence is shown in Figure 7.

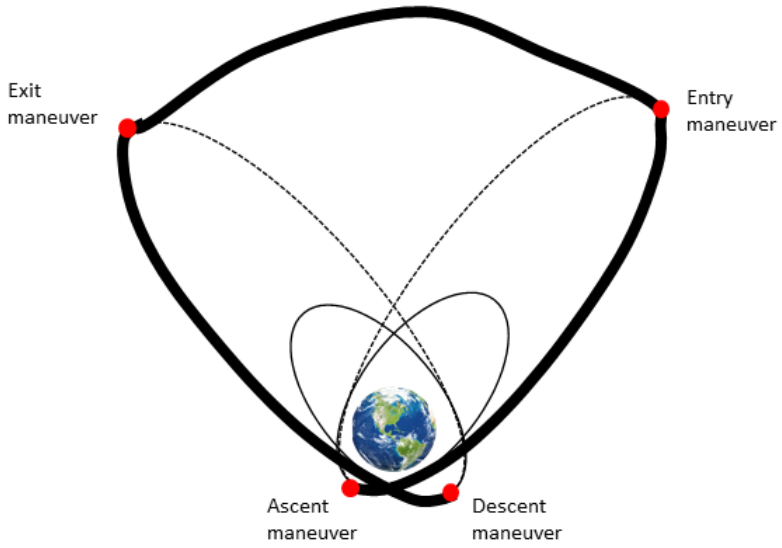

Figure 10: Notional trajectory produced by deep space reconfiguration maneuvers.

It should be noted that if the target locations and orbit period for observations are specified, there are four degrees of freedom in the maneuver sequence:

1. Total time allowed for the reconfiguration (0-90 days)
2. The period of the intermediate orbit (0-120 days)
3. The mean anomaly when the ascent maneuver is performed (0-360 deg)
4. The mean anomaly when the exit maneuver is performed (0-360 deg)

For preliminary analysis purposes, the minimum delta-v for a specified reconfiguration is computed by performing a global search across these variables.

The total delta-v cost of the reconfiguration maneuvers for a fully specified scenario is computed using the following four-step process:

1. The orbits required to observe each target are computed under the following assumptions:
    - The telescope has a latitude of 20deg.

- The velocity of the starshade perpendicular to the line of sight is equal to the velocity of the telescope perpendicular to the line of sight when the longitude of the telescope is equal to the longitude of the target.
- The velocity of the starshade along the line of sight is positive and set to achieve the specified observation orbit period.

2. The delta-v costs of the ascent and descent maneuvers are computed by taking the difference between the perigee velocity of the observation orbit and the intermediate orbit.
3. A Lambert solver [8, 9] is used to compute the velocities needed at the entry and exit points of the transfer arc. The time allowed for the transfer arc is computed by subtracting four quantities from the total reconfiguration time:
   - The time between the last observation and the ascent maneuver.
   - The time between the ascent maneuver and the entry maneuver.
   - The time between the exit maneuver and the descent maneuver.
   - The time between the descent maneuver and the next observation.
4. The delta-v costs of the entry and exit maneuvers are computed by taking the differences between the velocities of the intermediate orbits and the entry and exit velocities for the transfer arc.

First, it is necessary to characterize the sensitivity of the delta-v cost of an orbit reconfiguration to the angular distance between the targets. For simplicity, this is assessed for a reference scenario with a 15day observation orbit period. It is also assumed that the declination and right ascension of the first target star in this scenario are 30deg, and 0deg, respectively. The delta-v cost required to reconfigure the orbit to observe targets with different declinations and right ascensions are shown in Figure 11 (left). Figure 11 (right) instead shows the delta-v cost per degree separation between the targets. It is evident from these plots that for small angular separations (¡10 deg), the delta-v cost is approximately 20m/s per degree, in agreement with previous results. However, the cost per degree decreases by up to 33% for larger reconfigurations. Overall, it is evident from this plot that using the deep space reconfiguration approach can provide significant delta-v savings for large reconfigurations.

To further characterize the potential delta-v savings using the proposed strategy, simulations of large reconfigurations (>15deg) were repeated with observation orbit periods ranging from 4 to 20 days. The trade space between angular separation, observation orbit period, and delta-v cost of a reconfiguration is shown in Figure 12. For simplicity, it is assumed that the angular separation is simply a difference in declination between the targets. It is evident from Figure 12 (right) that cost increases linearly with the size of the reconfiguration regardless of the orbit period with a slope of approximately 10m/s per degree. Instead, the observation orbit period introduces

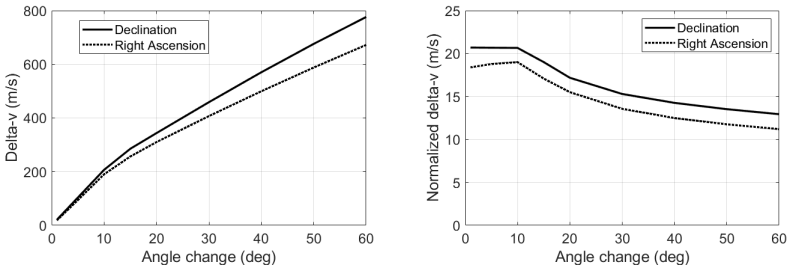

Figure 11: Reconfiguration delta-v vs angular separation (left) and delta-v cost per degree vs angular separation (right).

a constant bias in the delta-v cost. This behavior arises because small observation orbits require larger ascent and descent maneuvers to reach the optimal intermediate orbit (period between 60 and 90 days) that minimizes the delta-v cost of plane-change maneuvers. It is also evident that the sensitivity of the delta-v cost to the observation orbit period is largest for small orbits (see Figure 12 (left)). Specifically, the difference in the delta-v cost for an 8-day orbit and 20-day orbit is only 10%. Finally, the delta-v cost of a 60deg plane change is no larger than 800m/s provided that the observation orbit period is at least 12 days. While this does not meet the stated objective of 720m/s or less, it may be possible to meet this objective with more advanced maneuver planning tools.

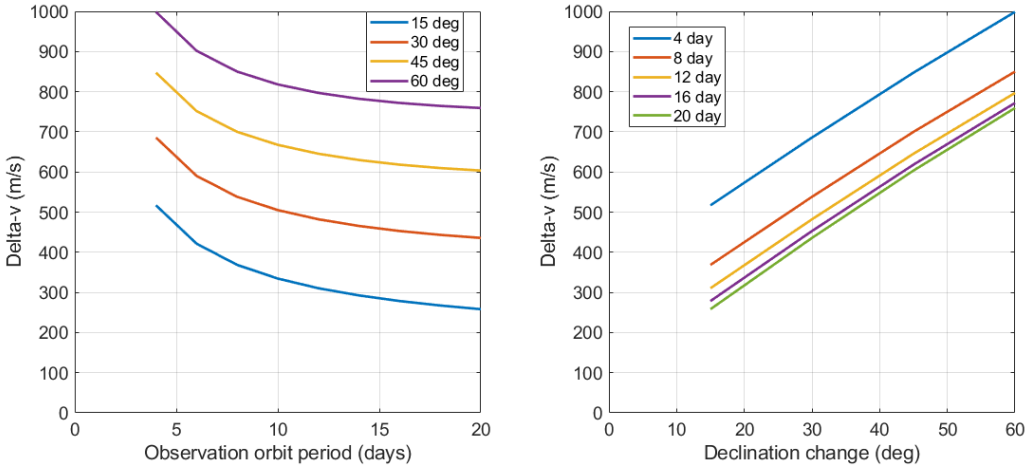

Figure 12: Delta-v cost of up reconfiguraiton vs angular separation and observation orbit period.

Overall, this analysis demonstrates that the suggested deep space reconfiguration approach can significantly reduce the delta-v required to reconfigure the starshade orbit to observe different targets with large angular separations. Indeed, the worst-case delta-v cost for a 60deg plane change for 4day observation orbit period is only 1km/s, which is 44% less than the cost of simply rotating the orbit. As such, use

of this approach can reduce the number of times the mission must be refueled and increase the frequency at which targets can be observed. Additionally, it is evident that the cost of formation reconfigurations is within an order of magnitude of the cost of station-keeping during observations ($\sim$300m/s to allow 3 observations per target), validating the claim that the propellant mass budget is dominated by the chemical propellant used for station-keeping during observations.

6 Distributed Mission Architecture Analysis

It is evident from the previous analysis that the total delta-v budget for the earth orbiting starshade mission will be at least 1km/s per observed target. To minimize the required propellant mass, the mission design includes a chemical propulsion to counteract the large relative accelerations between the starshade and telescope during observations and a SEP system for reconfiguration maneuvers (i.e. to ensure that the starshade is in the proper position for the next observation). Noting that the specific impulses for these systems differ by an order of magnitude, it was proposed to split the mission into two spacecraft: 1) a minimalistic starshade equipped with sufficient chemical propulsion to perform a single observation and 2) a servicer spacecraft that recovers the starshade, refuels it, and tows it to the required orbit for the next observation using SEP. The analysis in the following assesses the potential mass savings using this concept as well as its sensitivity to key variables such as spacecraft dry masses and specific impulses of the propulsion systems.

To quantitatively assess the propellant masses for chemical and electric propulsion systems, it is first necessary to define the operations concept for the mission using the distributed architecture. For simplicity, it is assumed that the operations concept includes the following steps which repeat for each observation:

1. The fully fueled starshade spacecraft separates from the servicer spacecraft.
2. The starshade spacecraft performs an observation maneuver using its chemical propulsion system (1hr duration), during which it negates the relative acceleration perpendicular to the line of sight from the ground-based telescope to the target star.
3. The servicer maneuvers to rendezvous with the starshade using the electric propulsion system.
4. The servicer docks with the starshade spacecraft and refuels it.
5. The servicer tows the starshade spacecraft to the orbit for the next observation.

For analysis purposes, these operations are reduced to a sequence of three maneuvers:

1. Observation maneuver performed by the starshade's chemical propulsion system (assumed to include delta-v required for separation and docking).
2. Rendezvous maneuver performed by the servicer's electric propulsion system (i.e. catching up to the starshade after the observation).
3. Tow maneuver performed by the servicer's electric propulsion system.

While the true delta-v costs of each of these maneuvers are complex functions of many variables (e.g. local solar time when observation is performed, latitude of telescope, location of target, etc.), many of these variables have minimal impact on

the total propellant mass allocation. To reduce the number of variables that must be considered, the following assumptions are adopted:

- All observation maneuvers have the same delta-v cost.
- The delta-v cost of a rendezvous maneuver is the same as the delta-v cost of an observation maneuver.
- The delta-v cost of a tow maneuver to observe the same target is the same as the delta-v cost of an observation maneuver.
- All tow maneuvers that configure the starshade to observe a different target have the same delta-v cost.

The propellant required for a maneuver is governed by the rocket equation, which is given by

$$\Delta v = g_0 I_{sp} \ln\left(\frac{m_s + m_f}{m_s}\right) \tag{23}$$

where g_0 is standard gravity (9.81m/s^2), I_{sp} is the specific impulse, m_f is the propellant mass expelled during the maneuver, and m_s is the mass of the rest of the spacecraft. Solving this equation for m_f yields

$$m_f = m_s\left(e^{\frac{\Delta v}{g_0 I_{sp}}} - 1\right) \tag{24}$$

The required propellant masses for the chemical and electric propulsion are estimated through simulations of a reference mission under the previously stated assumptions. Each simulation is executed in reverse order with an initial condition that the starshade and servicer are docked and all propellant is depleted. Propellant masses are added to each spacecraft as needed for each maneuver. Specifically, the order of operations for the simulation is given by

1. Increment electric propellant mass to account for rendezvous maneuver performed by servicer
2. Increment chemical propellant mass to account for observation maneuver performed by starshade
3. Increment electric propellant mass to account for tow maneuver performed by servicer docked with starshade (if not at the beginning of the mission)

Using this model, the propellant masses required for a reference mission can be computed deterministically as a function of eight variables, which include 1) number of targets, 2) number of observations for each target, 3) delta-v cost of an observation, 4) delta-v cost of towing the starshade to observe a new target, 5) dry mass of starshade spacecraft, 6) dry mass of the servicer spacecraft, 7) specific impulse of the electric

propulsion system, and 8) specific impulse of the chemical propulsion system. To assess the benefit of the distributed architecture, these simulations are repeated for a monolithic starshade spacecraft equipped with both chemical and electric propulsion. Parameters for the baseline reference mission are included in Table 1.

Starshade dry mass (kg)	7000
Servicer dry mass (kg)	5000
Monolithic dry mass (kg)	10000
Chemical Isp (s)	280
Electric Isp (s)	2800
Number of targets	4
Observations per target	3
Observation delta-v cost (m/s)	100
Different target tow delta-v cost (m/s)	800

Table 1: Reference mission parameters.

The propellant masses for this reference mission are given in Table 2.

	Distributed	Monolithic
Chemical propellant (kg)	3114	5841
Electric propellant (kg)	1990	1549
Total propellant (kg)	5104	7390

Table 2: Propellant masses for reference mission.

It is clear from these results that moving from the monolithic to the distributed architecture increases the required electric propellant but saves chemical propellant. Overall, this results in a 31% reduction in propellant mass even with a larger dry mass for the complete system. For reference, the sensitivity of the chemical, electric, and total (chemical + electric) propellant masses to key design variables are included in Figure 13. Several conclusions can be drawn from these plots. First, it is evident that a 40% increase in the dry mass of the servicer increases the total propellant mass by only 7% (all of which is electric propellant). This sensitivity is much less than for the monolithic case, where the propellant mass is proportional to the dry mass of the spacecraft. Due to the diminished sensitivity to dry mass, it may be beneficial to add additional electric thrusters to the servicer because the corresponding reduction in the time required for orbit reconfigurations justifies the small increase in required propellant mass. Second, a 25% increase in the delta-v cost of a tow maneuver increases the total propellant mass by 7% (all of which is electric propellant). This confirms that the total propellant budget is dominated by chemical propellant unless the delta-v cost of a tow maneuver is drastically increased ($\geq$2km/s). Third, the total propellant mass is most sensitive to changes in the specific impulse of the chemical propulsion system. Accordingly, this should be maximized. Increasing the specific impulse of the electric propulsion system can also reduce system mass, but this is

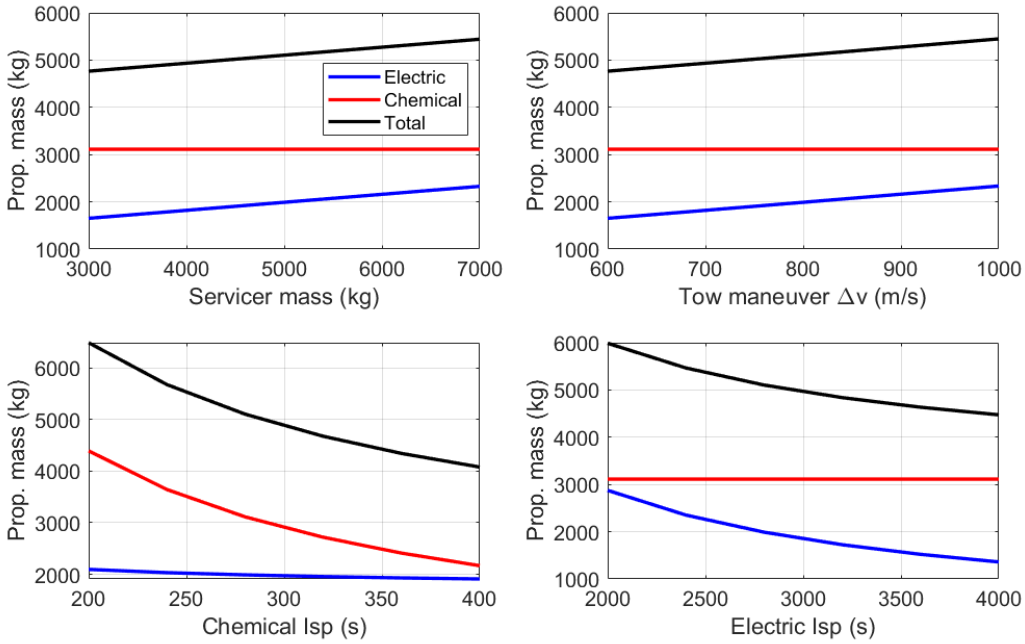

Figure 13: Propellant mass sensitivities to design variables.

constrained by available technologies and the need to achieve sufficient thrust to perform rendezvous and tow maneuvers in an acceptable time. Finally, the largest total propellant mass for the considered parameter ranges is 6488 kg, which is still nearly one ton less than the propellant required for a monolithic spacecraft with nominal mission parameters. Thus, it is clear that the distributed mission architecture significantly reduces the required propellant mass and reduces the sensitivity of the propellant mass to key mission parameters.

7 Conclusions

This technical note addressed orbit design and control challenges for a formation consisting of an earth-orbiting starshade and ground-based telescope intended to image earth-like exoplanets, producing several important findings.

First, it was demonstrated that the delta-v cost of station-keeping during an observation can be computed analytically as a function of the telescope latitude, the target declination, and the time and duration of the observation. The delta-v cost increases with the absolute value of the target declination and the cosine of the telescope latitude. However, this delta-v cost is bounded by the centripetal acceleration of the telescope and cannot exceed 121m/s per hour of observation in any configuration. Also, to enable such large maneuvers in a short time with a low thruster duty cycle, the starshade must be equipped with chemical propulsion with 7000N thrust. To minimize delta-v costs while ensuring that the optical constraints are satisfied, observations should be conducted as close as possible to the hour following 7:15PM or preceding 4:45AM.

Second, it was demonstrated that the telescope latitude and time of observation must be selected to ensure that the starshade always has a perigee orbit altitude of at least 1000km. To meet this requirement, the telescope latitude can be no larger than 35 degrees. Additionally, it was found that the observation window for near-equatorial targets is only a few hours in duration regardless of telescope latitude. Accordingly, targets for the mission should be carefully selected to ensure sufficient revisit opportunities (favoring polar targets) while minimizing delta-v consumption (favoring near-equatorial targets).

To allow the starshade to align with different targets with large angular separations, a novel deep space reconfiguration approach was proposed and analyzed. It was demonstrated through simulation that this approach enables plane changes of up to 60deg at delta-v costs of under 1km/s for all feasible observation orbit periods, providing a savings up to 44% compared to simply rotating the observation orbit.

Finally, an analysis was conducted to characterize the potential of using a distributed architecture consisting of a minimalistic starshade spacecraft and large servicer carrying the required propellant. It was found that this architecture provides a propellant mass savings of over two tons for a reference mission profile even though the dry mass of the total system is larger. Additionally, it was found that the sensitivity of the total propellant mass to mission parameters such as dry mass is significantly reduced for the distributed architecture. The latter property suggests that the electric propulsion can be increased to reduce reconfiguration times with a negligible impact on the required propellant.

The results of this analysis suggest that several topics should be studied in more detail in future work. First, a design reference mission should be developed to enable validation of key assumptions (e.g. separation between targets) and more accurate

computation of delta-v and propellant mass budgets. Second, it is necessary to develop a low-thrust maneuver planning algorithm, which can be used to characterize the trade space between delta-v cost and allowed time for reconfiguration maneuvers at various thrust levels. Finally, effects of perturbations by the sun, moon, and solar radiation pressure as well as navigation and control errors need to be assessed. The lunar perturbation is of particular interest as it can be exploited to perform large orbit reconfigurations at reduced delta-v cost.

8 References

[1] A. W. Koenig, S. D'Amico, B. Macintosh, and C. J. Titus, "A Pareto-Optimal Characterization of Small-Scale Distributed Occulter/Telescope Systems," *Optical Engineering + Applications*. San Diego, CA, USA, 2015.

[2] A. W. Koenig, B. Macintosh, and S. D'Amico, "Formation Design of Distributed Telescopes in Earth Orbit for Astrophysics Applications," *Journal of Spacecraft and Rockets*, Vol. 56, No. 5, 2019, pp. 1462–1477.

[3] A. W. Koenig, *Formation Design of Distributed Telescopes in Earth Orbit with Application to High-Contrast Imaging*. PhD thesis, Stanford University, 2019.

[4] S. D'Amico, A. Koenig, B. Macintosh, and D. Mauro, "System Design of the Miniaturized Distributed Occulter/Telescope (mDOT) Science Mission," *33rd Annual Conference on Small Satellites*. Logan, UT, USA, 2019.

[5] A. W. Koenig, S. D'Amico, B. Macintosh, and C. J. Titus, "Optimal Formation Design of a Miniaturized Distributed Occulter/Telescope in Earth Orbit," *2015 AAS/AIAA Astrodynamics Specialist Conference*. Vail, CO, USA, 2015.

[6] A. W. Koenig, S. D'Amico, B. Macintosh, and C. J. Titus, "Formation Design Analysis of a Miniaturized Distributed Occulter/Telescope in Earth Orbit," *25th International Symposium on Space Flight Dynamics*. Munich, Germany, 2015.

[7] A. W. Koenig and S. D'Amico, "Fast Algorithm for Energy-Optimal Impulsive Control of Linear Systems with Time-Varying Cost," *IEEE Transactions on Automatic Control*, 2019. Submitted.

[8] R. C. Blanchard and E. R. Lancaster, "A unified form of Lambert's theorem," NASA Technical Note TN D-5368, 1969.

[9] R. H. Gooding, "A procedure for the solution of Lambert's orbital boundary-value problem," *Celestial Mechanics and Dynamical Astronomy*, Vol. 48, No. 2, 1990, pp. 145–165.